FIFTH AUSTRALASIAN CONFERENCE

on

HYDRAULICS AND FLUID MECHANICS

at

University of Canterbury, Christchurch, New Zealand
1974 December 9 to December 13

BOUNDARY LAYER WALL-PRESSURE FLUCTUATIONS NEAR AN ABRUPT CHANGE IN SURFACE ROUGHNESS

by

P.J. Mulhearn*

SUMMARY

The wall-pressure fluctuations beneath a turbulent boundary layer have been investigated immediately downstream from an abrupt change in surface roughness, the change being from a slightly-rough to a very-rough surface. The r.m.s. pressure decreases slightly at first, then rises to a peak value about 250 mm from the change in surface roughness before decreasing once more. Pressure spectra for a range of free-stream velocities and at various stations in the first 150 mm scale on wall variables. Further downstream this behaviour breaks down.

The internal layer which grows from the start of the new rough surface ceases to have a distinct edge at about the position of the peak in the r.m.s. pressure. This peak may be associated with the change from a thin internal layer dominated by wall variables to a more complex flow resulting from the interaction of this internal layer with the upstream boundary layer once the former has reached a certain thickness.

*Division of Environmental Mechanics, CSIRO, P.O. Box 821, Canberra City, A.C.T. 2601, Australia. This paper reports on work done while the author was with the Royal Australian Navy Research Laboratory, Sydney.

INTRODUCTION

The pressure fluctuations imposed by a turbulent boundary layer on the surface beneath it are of interest for a number of reasons. If the surface is a ship's hull, or sonar dome, these pressure fluctuations act as an unwanted source of background noise and often set up vibrations in the hull, increasing radiated noise and on occasion loosening plates. It has also been suggested that surface pressure fluctuations beneath the atmospheric boundary layer may be significant for air movements in very porous soils and within dense plant canopies.

Much work has been done on fully-developed boundary layers on both smooth (1,2) and rough walls (3,4). However, turbulent wall-pressure fluctuations are still not fully understood and it was felt that an investigation of the effects of an abrupt change in surface roughness would provide fresh insight into this phenomenon. In addition, many rough surfaces do not have sufficient upstream fetch of uniform roughness for a fully-developed boundary layer to form, so that the severely non-uniform case considered here is again of interest.

EQUIPMENT AND PROCEDURES

The experiments were performed in the 1.83 m x 0.61 m open-return blower wind tunnel of the Division of Environmental Mechanics, CSIRO, Canberra (5). The author used this facility for two weeks late in August 1973 and returned for two more days in October 1973. The pressure-measuring equipment used differed on the two occasions.

The boundary layer was formed on the floor of the working section with the adjustable roof set for zero pressure-gradient. The first 3 m consisted of undressed ply-wood in 0.61 m sheets, followed by 3 m of a rough surface formed by slots 9.5 mm wide, 3.6 mm high and 12.7 mm apart spanning the tunnel, as shown in Figure 1.

The arrangement was very similar to that used by Antonia and Luxton (6), hereafter cited as AL, the main difference being that a much wider working section was used in the present experiments (1.83 m as against 0.38 m), and the upstream surface was slightly rough rather than smooth. This scheme was used because limited time was available for the experiments, and the turbulent velocity structure and wall shear-stress behaviour could then be considered known.

Mean velocities were measured with a boundary-layer pitot tube and an inclined manometer. Turbulent shear stress and mean square velocity fluctuations were measured with an X-wire probe and Disa 55D01 constant temperature anemometers.

Wall-pressure fluctuations were measured in the first series of experiments with the following Bruel and Kjaer equipment: a 4138 3.2 mm microphone, a 4136 6.4 mm microphone, a 2615 cathode follower, and a 2112 spectrum analyser. The sensing areas of the microphones were reduced by mounting them in plugs in which a 0.80 mm pin-hole was drilled. The appropriate plug was then inserted in the wall between roughness elements, as shown in Figure 2. The spectrum analyser was used for a few measurements only and most data were recorded for later analysis.

In the second series, a 4135 6.4 mm microphone and a battery-operated 2630 cathode follower were used. The microphones were mounted in a hole, terminated by a 0.80 mm pin-hole, in the wall itself. Measurements were obtained both on slot centre-lines and on the centre-lines of roughness elements. It was later realised that a low frequency roll-off at about 400 Hz was imposed by the battery-operated cathode follower and so only data for frequencies higher than that are presented from the second series of experiments.

Free-stream mean velocities between 20.4 and 28.4 m/sec were used in these experiments. These are higher than those used by AL and avoided background noise problems at lower velocities (see below).

LIMITATIONS ON MEASUREMENTS OF PRESSURE FLUCTUATIONS

The measurements were limited at the high frequency end of the power spectrum by the spatial resolution of the pin-hole microphone. Corcos (7) has estimated that a +3 dB correction to the measurements is required when

$$\omega d/2\, U_{cp} \simeq 1,$$

where ω = radian frequency,
d = sensing area diameter, and
U_{cp} = phase velocity of the pressure fluctuations.

For most of the measurements presented here this corresponds to a frequency of 7 kHz. The resonant frequency of the cavity between the pin-hole and the microphone face was calculated as 9 kHz,

though no resonant peak was detected.

The low frequency limit was set by the background noise level. The wind-tunnel air speed was controlled by vanes at the fan inlet. Thus, the noise measured with the microphone in the measuring station, the inlet vanes closed, the fan running, and negligible air flow, could be taken as the background. Measurements at various places within the tunnel room indicated that at most frequencies the background noise with the vanes closed was slightly greater than that with the vanes opened. This conclusion was supported by measurements with the pin-hole blocked and the microphone in position in the rough wall. It was concluded that the signal was at least 10 dB above background noise for free-stream speeds above 25 m/sec and for frequencies above 160 Hz on the very rough wall, except for a strong resonance at 630 Hz probably due to standing sound waves in the tunnel. However, this occurred at a quite discrete frequency and was only apparent at one station . It could easily be distinguished. At 20.4 m/sec the frequency band with an acceptable signal-to-noise ratio was more limited; hence the few points presented for this free-stream speed.

The usable frequency range for speeds above 25 m/sec was therefore 160 Hz to 7 kHz. As noted earlier, the low frequency roll-off of the instrumentation in the second series of experiments was at about 400 Hz. Broad-band estimates of r.m.s. pressure were, however, obtained for the range 160 Hz to 7 kHz in these experiments. The error was not large, because the roll-off was not sharp.

RESULTS AND DISCUSSION

(a) Mean flow and velocity fluctuations

Because in both these experiments and those of AL the same rough surface was used downstream from the abrupt roughness transition and the flow was fully rough, the variation in skin friction coefficient C_f and the thickness δ_i of the associated internal boundary layer, should be independent of Reynolds number. Hence, only sufficient mean and turbulent velocity measurements were taken to verify that the rough-wall boundary layer flow behaved substantially the same as that of AL. The only major difference was that turbulent shear stresses measured in these experiments were 10-20% higher than those of AL, who think, however, that their measurements might be too low.

AL also measured the skin friction coefficient, C_f, in the non-equilibrium region just downstream of the transition, using pressure-tapped roughness elements. The use of mean velocity profiles for this purpose is inapplicable in this rapidly changing region. In view of the close correspondence between the two flows their complete and careful measurements for C_f and δ_i, shown on Figure 3, can be applied to the analysis of pressure spectra presented below. C_f on the upstream rough surface was 0.0031 and was 0.0083 well downstream, while the equivalent sand grain roughness changed from 0.125 mm to 17.8 mm.

(b) Wall-pressure spectra

Measurements of wall-pressure spectra were obtained on the first 300 mm of the very rough surface, at the stations indicated in Figure 3, and well downstream at 2170 mm. In the region immediately downstream from the change in surface roughness AL's velocity profiles indicate that there is a clearly-defined internal layer, but by 300 mm downstream the edge of the layer has become indistinct. The pressure fluctuation measurements are thus concentrated in this transition region.

Some of the measurements taken on slot centre-lines at a free stream speed of 28.2 m/sec are shown in Figure 4, where f is circular frequency, $\Phi(f)$ is defined such that the mean square pressure fluctuation $\overline{p^2}$ is given by

$$\overline{p^2} = \int_0^\infty \Phi(f)\,df,$$

and X_1 is distance downstream from the roughness change. It can be seen that spectra taken within the first 150 mm have a pronounced peak at about 250 Hz and their high frequency energy decreases with distance downstream. However, at 248 mm the energy at higher frequencies has increased and there is no peak at 250 Hz.

In Figure 5, the spectra taken on slot centre-lines in the first 150 mm at a free stream speed of 28.2 m/sec are shown non-dimensionalised on roughness element height (or slot depth), h, wall shear stress, τ_w, and friction velocity, $U_\tau = (\tau_w/\rho)^{\frac{1}{2}}$. In this and subsequent figures, $\Phi(\omega)$ is defined such that

$$\overline{p^2} = 2\int_0^\infty \Phi(\omega)\,d\omega.$$

It can be seen that the spectra scale well on these variables for all frequencies except at the peak. The reason for poor scaling there is not understood. There is, however, a slight trend for the non-dimensionalised spectral values to increase with distance downstream. Note that the spectra appear to increase as ω^2 at low frequencies. In Figure 6, spectra non-dimensionalised in the same way are shown for various free-stream speeds for the slot centre-line at 43 mm and the roughness element centre-line at 50 mm from the start of the new rough surface (i.e. the fourth slot and roughness element, respectively). The collapse of the data is excellent. The shapes of the spectra clearly differ for the two stations. When the spectra of Figure 5 were nondimensionalised using δ_i, the thickness of the internal layer, instead of h as length scale, the spread of the data was large.

Spectra measured at stations further downstream on slot centre-lines are illustrated in Figure 7. It can be seem that the collapse of the data is poor and that the spectral levels, at all frequencies measured, increase to a maximum at 248 mm downstream and then decrease. At the low frequency end the difference between 146 mm and 248 mm is quite pronounced, the enhanced low-frequency spectral levels being maintained well downstream as indicated by the broken line representing the 2170 mm data.

Spectra for the slots at 248 mm and 299 mm, at various free-stream speeds, are illustrated in Figure 8. A trend for the non-dimensional spectral values to increase with decrease in speed is evident at 299 mm. The same general picture was obtained using free-stream speed and dynamic head and overall boundary-layer thickness as scaling parameters.

All spectra were also non-dimensionalised using various combinations of h, δ_i, U_τ, τ_w, and U_o, the free-stream velocity. When these schemes were tried on spectra at <u>different locations</u>, the spread of data was very <u>markedly increased</u> compared to the spread of the raw dimensional spectra of Figure 4.

In the first 150 mm of the rough surface there is thus a region in which the wall-pressure fluctuations scale reasonably well on wall variables and are presumably mainly generated by motions very close to the roughness elements. This is supported by the decrease of spectral level ($\Phi(\omega) \propto \omega^2$) for frequencies below 250 Hz. In the same region, Antonia and Luxton (8) measured turbulent velocity and shear-stress spectra. They found that in the outer part of the internal layer the spectra scaled on the turbulent shear stress, τ, and δ_i, while close to the wall, spectra scaled on τ and the distance from the wall, z. This again suggests that the wall-pressure fluctuations in this region are mainly generated by motions very close to the wall.

Beyond 150 mm the behaviour is more complex. It may be that upstream from 150 mm the internal layer behaves as a separate entity, while beyond 150 mm, as the scale of the internal layer grows, it is able to interact with the turbulent flow outside it and so fluctuations close to the walls are increasingly modified by motions with which they were previously unrelated.

The motions further from the wall, but within the internal layer, may be responsible for the slight increase with distance downstream in the non-dimensional levels of Figure 5.

Well downstream, at 2170 mm from the roughness change, where a fully-developed boundary layer exists, spectra were obtained on the centre-lines of both a slot and a roughness element for several free-stream speeds. These are shown in Figure 9, non-dimensionalised on wall variables. Equally good collapse was found using the outer flow variables - boundary-layer thickness, free-stream velocity, and free stream dynamic head. This indicated that motions in the outer part of the boundary layer are in equilibrium with the wall shear stress, as would be expected far downstream. As at 300 mm (see Figure 8), there is a slight increase in spectral level with decrease in free-stream speed. The difference in the shape of the spectra between slot and roughness element is not as marked as that found further upstream (Figure 6).

(c) <u>Root mean square pressure fluctuations</u>

The variation of r.m.s. pressure, p', and p'/τ_w with distance downstream from the step-change in surface roughness is shown in Figure 10. If the spectra scaled exactly on wall variables at all frequencies, p'/τ_w would be a constant. Some of the change in the first 150 mm is due to the difference in level at the 250 Hz peak, where the scaling did not work, and some is due to a gradual increase at all frequencies. The slight initial decrease followed by a rise in r.m.s.pressure up to 250 mm and subsequent decrease is apparent. It is not known if more fluctuations in $p'(x_1)$ occur further downstream, but such behaviour would be unlikely. The ratio p'/τ_w is 1.45 well downstream. This is considerably less than the value of 3.8 to 2.9 found by Blake (3) for walls with sand-grain roughness. The difference is due in part to a need to high-pass filter at 160 Hz in the present experiments.

CONCLUSIONS

Immediately downstream from an abrupt change from a slightly- to a very-rough surface the spectra of wall-pressure fluctuations beneath a turbulent boundary layer scale on wall variables. This and other considerations indicate that the motions generating the pressure fluctuations are very close to the surface.

Further downstream this behaviour begins to break down, and there is a maximum in r.m.s. pressure at 248 mm from the roughness change. It may be that in the initial region the intense internal layer is too small in scale to interact appreciably with the external flow. However, as its thickness increases it does interact and the simple initial behaviour is modified.

ACKNOWLEDGEMENTS

Thanks are due to Dr I. Seginer of the Agricultural Engineering Faculty, Technion, Haifa, Israel, who was visiting the Division of Environmental Mechanics, CSIRO, Mr J. Finnigan of the same CSIRO Division, and Messrs B. Maddaford and F. Bruzzone of the R.A.N. Research Laboratory for their help with these experiments. Dr Seginer and Mr Finnigan also made most of the mean and turbulent velocity measurements. Thanks are due also to Dr M.K. Bull and Professor R.E. Luxton of Adelaide University for some helpful discussions and the loan of equipment and to Drs J.R. Philip and E.F. Bradley for use of the Pye wind tunnel.

REFERENCES

(1) Willmarth, W.A. and Wooldridge, C.E. (1962). J. Fluid Mech. 14, 187.
(2) Bull. M.K. (1967). J. Fluid Mech. 28, 719.
(3) Blake, W.K. (1970). J. Fluid Mech. 44, 637.
(4) Aupperle, F.A. and Lambert, R.F. (1968). J. Acoust. Soc. Amer. 47, 359.
(5) Wooding, R.A. (1968). Aust. CSIRO Div. Plant Ind. Tech. Pap. No. 25. 39 pp.
(6) Antonia, R.A. and Luxton, R.E. (1971). J. Fluid Mech. 48, 721.
(7) Corcos, G.M. (1963). J. Acoust. Soc. Amer. 35, 192.
(8) Antonia, R.A. and Luxton, R.E. (1973). Dept. Mech. Eng., Univ. of Sydney, Charles Kolling Res. Lab. Tech. Note F-55. 39 pp.

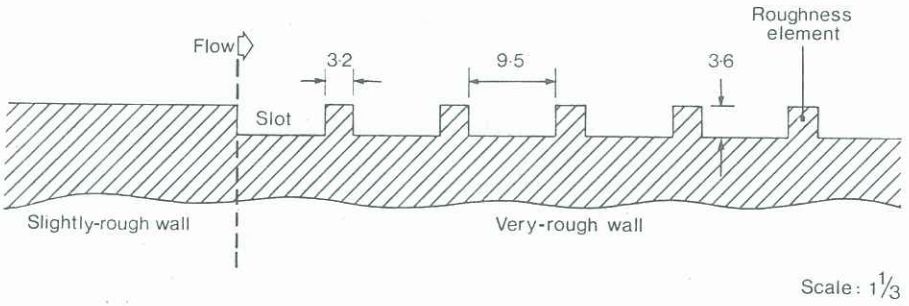

Figure 1. Geometry of surface (dimensions in mm).

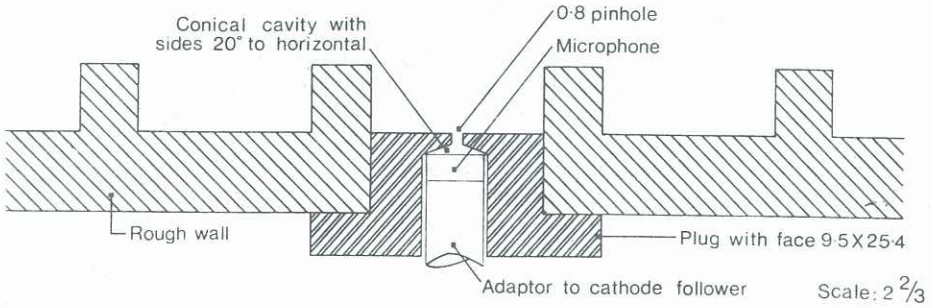

Figure 2. Geometry of pin-hole microphone.

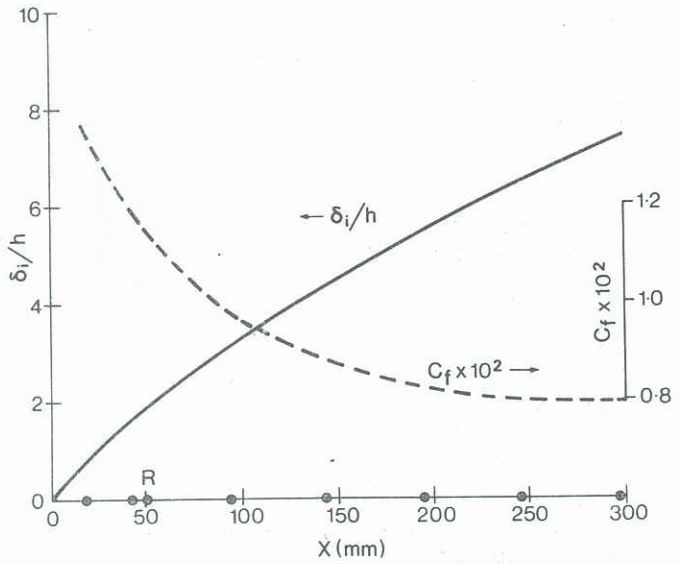

Figure 3. Curves through experimental values of C_f and δ_i, from Antonia and Luxton (6), and positions of measuring stations, ⊛ . That labelled R is at roughness element centre-line; the others are at slot centre-lines.

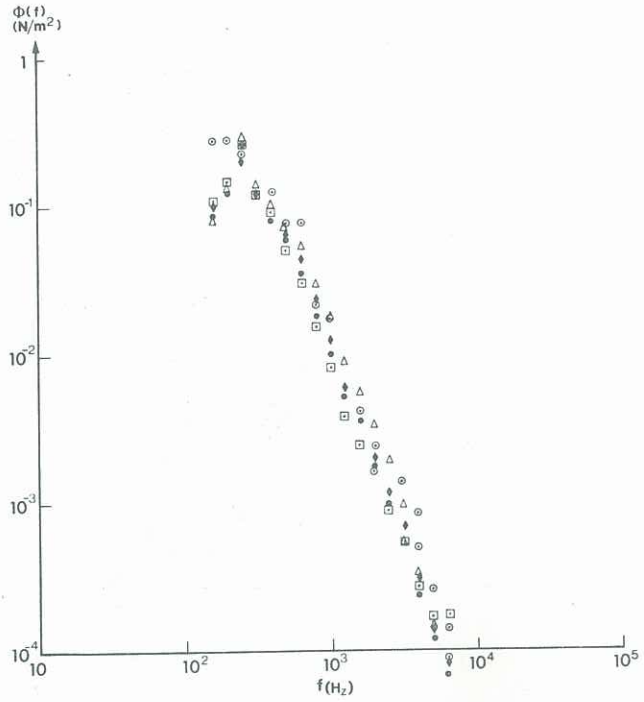

Figure 4. Wall-pressure spectra from slot centre-lines near change in roughness at 28.2 m/sec for X_1 stations indicated: △ , 17.5 mm; ♦ , 43 mm; ● , 94 mm; ⊡ , 146 mm; ⊙ , 248 mm.

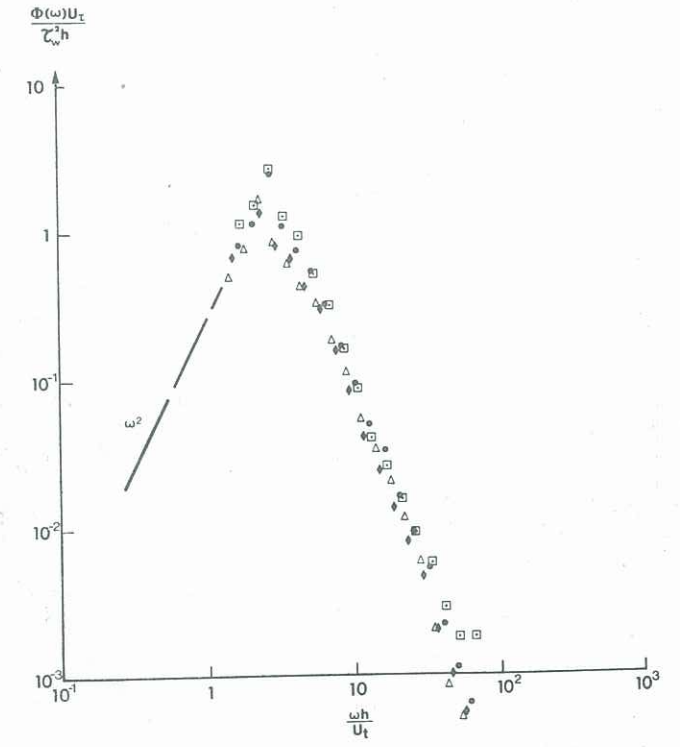

Figure 5. Non-dimensional wall-pressure spectra from slot centre-lines on first 150 mm of very-rough surface at 28.2 m/sec, for X_1 stations indicated: △ , 17.5 mm; ♦ , 43 mm; ● , 94 mm; ⊡ , 146 mm.

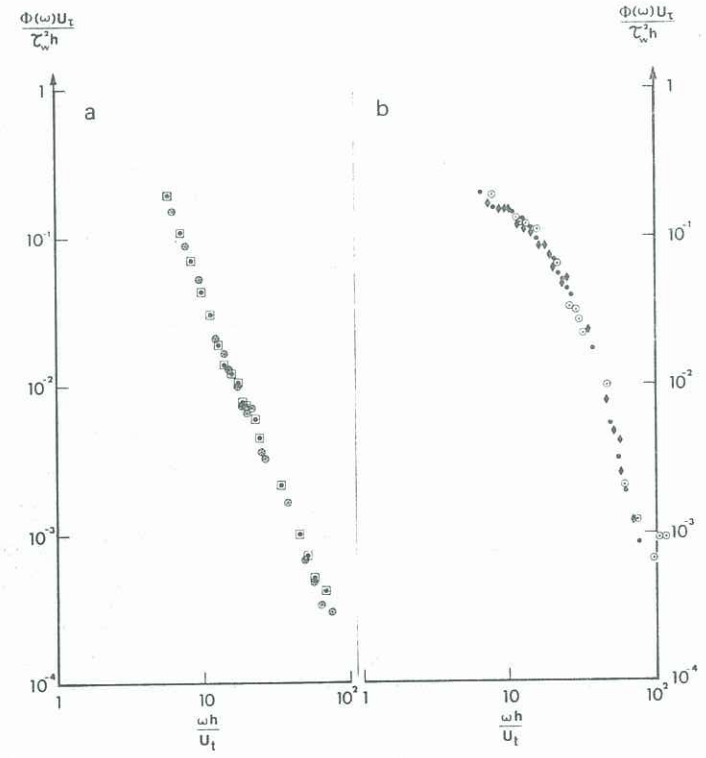

Figure 6(a). Wall-pressure spectra from slot at 43 mm for free-stream speeds shown: ⊛ , 28.2 m/sec; ⊛ , 25.8 m/sec.

(b). Wall-pressure spectra from top of roughness element at 50 mm for free-stream speeds shown: ♦ , 28.2 m/sec; ◍ , 25.8 m/sec; ⊙ , 20.4 m/sec.

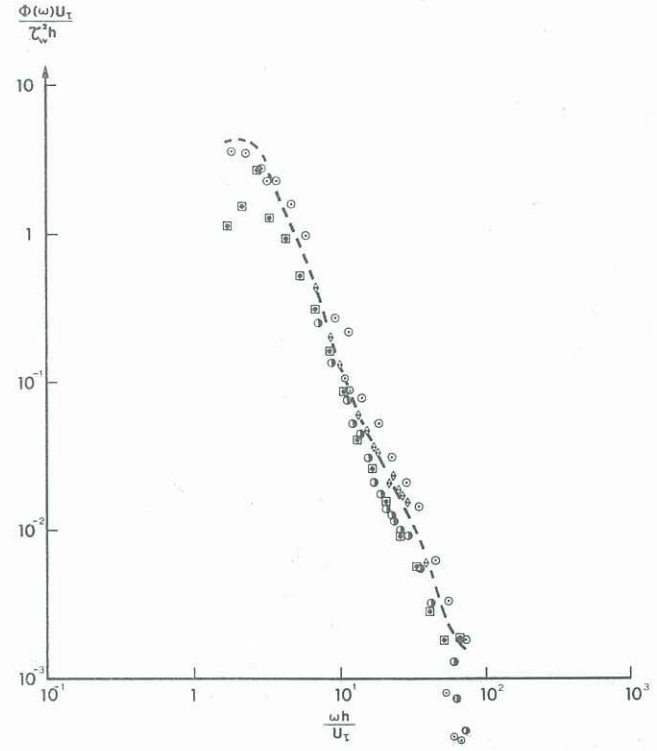

Figure 7. Wall-pressure spectra from slots downstream from 150 mm for a free-stream speed of 28.2 m/sec: ◙ , 146 mm; ◈ , 197 mm; ⊙ , 248 mm; ◑ , 299 mm; - - - -, 2170 mm.

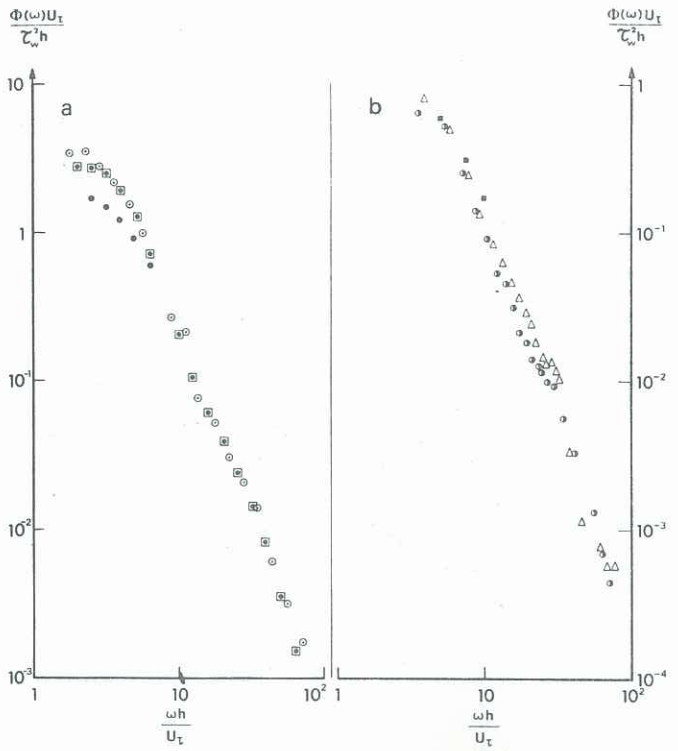

Figure 8. Wall-pressure spectra from slots at (a) 248 mm, and (b) 299 mm.
(a) ⊙ , 28.2 m/sec; ◙ , 25.8 m/sec; ● , 20.4 m/sec.
(b) ◑ , 28.2 m/sec; △ , 25.8 m/sec; ■ , 20.4 m/sec.

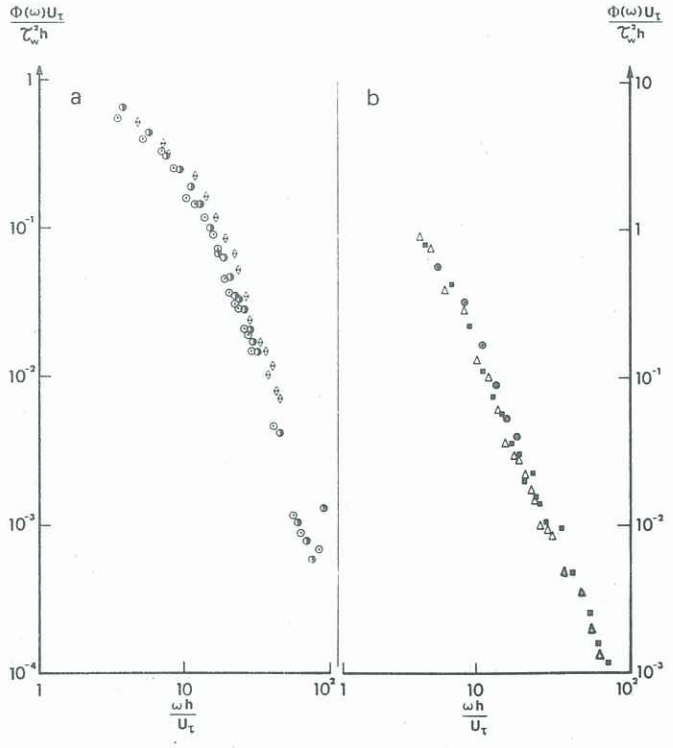

Figure 9. Wall-pressure spectra well downstream at 2170 mm, (a) from roughness-element centre-line, and (b) from slot.
(a) ⊙ , 28.2 m/sec; ◑ , 25.8 m/sec; ◈ , 20.4 m/sec.
(b) △ , 28.2 m/sec; ■ , 25.8 m/sec; ⊛ , 20.4 m/sec.

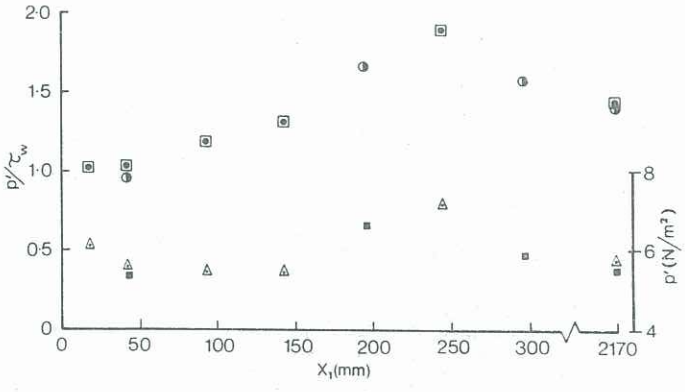

Figure 10. Streamwise development, above 160 Hz, of p' (△, ■) and p'/τ_W (◙, ◑). 1st series: ◙, △ . 2nd series, with slow low-frequency roll off at about 400 Hz: ◑ , ■ .